Ann. Geophys., 28, 665–676, 2010
www.ann-geophys.net/28/665/2010/

Annales Geophysicae

Comment on "Global structure, seasonal and interannual variability of the migrating semidiurnal tide seen in the SABER/TIMED temperatures (2002–2007)" by Pancheva et al. (2009)

A. Manson, C. Meek, and X. Xu

Institute of Space and Atmospheric Studies, University of Saskatchewan, Saskatoon, Canada

Received: 13 August 2009 – Revised: 3 February 2010 – Accepted: 19 February 2010 – Published: 25 February 2010

1 Introduction

In a recent paper, Pancheva et al. (2009, hereinafter referred to as PETAL09) discussed the altitude (70–120 km) and latitude (50° S–50° N) structures, seasonal and interannual variability of the migrating thermal semidiurnal tide (SDT) derived from the SABER/TIMED temperature measurements. In their "Discussion and summary" (Sect. 4) just before the summary is provided, and regarding the comparison between the thermal SDT characteristics at middle latitudes (∼40° N) derived from SABER temperatures and those derived from Na lidar observations over Fort Collins, Colorado (41° N, 105° W) reported by Yuan et al. (2008, hereinafter referred to as YETAL08), PETAL09 made a number of statements that caused us serious concern: *"(iii) the vertical wavelength found by the lidar is ∼50 km in most of the months with the exception of the summer months when it is longer; in June however the tidal phase was almost independent of height indicating that the semidiurnal tide is evanescent or with very large vertical wavelength. The SABER tidal wavelengths at 40 N however are different from the lidar ones; they indicate slight seasonal variability and on the average their magnitudes are clustered near 35 km. This significant difference between the lidar semidiurnal tide observed over Fort Collins and the SABER tide at 40 N defines a different contribution of the Hough modes; while for the lidar semidiurnal tide the Hough modes with very long vertical wavelengths (2, 2) and (2, 3) are dominant in summer the SABER tide is composed by modes with significantly shorter wavelength as (2, 4) and (2, 5) modes.*" In contrast there are numbers of published studies, using radar observations, which agree with those from Fort Collins i.e. the summer wavelengths 80–100 km are significantly larger than in winter. Also there is the challenging notion that sampling of different Hough modes by the lidar and the satellite system SABER explains differences between the derived vertical wavelengths of the tides. This supposition also demands thought and discussion, since providing both systems have adequate height and horizontal resolution, the observed vertical wavelengths should not be system-dependent.

Later in their Summary of main results, and in its first paragraph, they state that, based upon their analysis of the SABER/TIMED temperatures, the "*seasonal behaviour of the semidiurnal tide [migrating] in the middle latitudes (+/−40 degrees) is dominated by a strong annual variation with a winter maximum in the upper mesosphere (90 km)....*" However, a close comparison between Fig. 1 of YETAL08 and Fig. 2 of PETAL09 provides the following difference: at altitudes of ∼90 km, the lidar thermal tidal amplitudes for Fort Collins show two maxima during the equinoctial periods of February–March and September–October, indicating an additional semi-annual modulation, whereas the SABER thermal tide (a hemispheric fit at 40° N) exhibits only a strong annual oscillation with a winter maximum.

Continuing on the theme of seasonal behavior of the migrating SDT at mid-latitudes (40° N and 40° S), PETAL09 stated later in their first Summary paragraph that "*For altitudes between 70 and 90 km besides the winter maximum an autumn (September in the NH and March in the SH) tidal amplification is evident as well. The September maximum detected at northern middle latitudes is well documented by radar studies (Manson et al., 1999, 2002a; Riggin et al., 2003)*". After re-examination of the upper left plot of

Correspondence to: A. Manson
(alan.manson@usask.ca)

Published by Copernicus Publications on behalf of the European Geosciences Union.

their Fig. 2, however, one finds that between 70 and 90 km a "September" tidal enhancement for 40° N is not evident; there is slight asymmetry at 70–80 km, with larger amplitudes for the months before December [August–November] than the months after [January–April]. Also in their Fig. 3 showing time sequences for six years, appropriate to 40° N at 90 km, there is no indication of the September maximum. The second sentence of their statement also indicates that PETAL09 did not make any possible distinctions between the features of the migrating SDT in the temperature and wind fields.

Therefore, it appears that PETAL09 has underestimated the differences between the mesospheric/mesopause semidiurnal (SD) tidal characteristics at middle latitudes 40–50° N derived from the SABER temperatures and those, especially dynamic characteristics (wind perturbations), revealed by other data sets (radars, lidars and models). We will show supporting evidence for this. Thus, the aim of this Comment is to correct some impressions about the wind and temperature tidal features at middle northern latitudes (∼40–50° N) provided by PETAL09, and to raise related questions or issues. In Sect. 2 there is a summary of the alternate systems used for SDT studies and their general and published findings; Sect. 3 and Sect. 4 will provide new tidal figures from ground-based observations and model data; and conclusions will be given in Sect. 5.

2 Background

There are usually three systems used to extract tidal information: ground-based observations (Medium Frequency (MFR), Meteor Wind Radar (MWR) and lidar), satellite observations and model studies. Manson et al. (1999) presented tidal winds (Diurnal Tide (DT) and SDT) in the height range of typically 75–95 km from 6 MF radars, located between the equator and high northern latitudes: Christmas Island (2° N), Hawaii (22° N), Urbana (40° N), London (43° N), Saskatoon (52° N) and Tromso (70° N), and compared the tidal amplitudes, phases, and wavelengths with seasonal Global Scale Wave Model (GSWM, 1995) values. This model is a 2-D linearized model that solves the Navier-Stokes equations for the tidal and planetary wave perturbations. An extended paper (Manson et al., 2002a), incorporating additional mid-latitude MFRs (Yamagawa 31° N, and Wakkanai 45° N) provided comparisons with the monthly values from GSWM 2000: the significant improvements to the model involve the use of UARS-HRDI data (High Resolution Doppler Interferometer), and monthly variations in the Rayleigh friction. The main seasonal characteristics of the SDT-wind observed with the MFR were reproduced in the two GSWM versions. The radar SDT observations were then compared with the General Circulation Model CMAM (Canadian Middle Atmosphere Model) without interactive chemistry (Manson et al., 2002b), and finally with CMAM with interactive chemistry, in comparison with the MFR data (Manson et al., 2006). For the latter paper, CMAM provided the main characteristics of the observed DT and SDT in the Northern Hemisphere, and quite detailed agreement with observations for the SDT at middle latitudes.

Briefly, consistent with the above papers, the following SDT-wind features were modeled (CMAM) and observed using radars in the CUJO network (Canada, United States, Japan Opportunity) and at Tromso:

1. for the middle to high-latitudes (Platteville, USA (40° N, 105° W); London Canada (43° N, 81° W); Wakkanai Japan (45° N, 142° W); Saskatoon Canada (52° N, 107° W); Tromso Norway (70° N, 16° E)), there is a dominant late-summer/early-fall maximum (LSEF) at altitudes of ∼75–97 km, a winter maximum at ∼85–97 km and an accompanying strong minimum during late-October to November;

2. from the three forty-degree MF radars, there is dominance of the migrating tidal wind in the region of late-summer/fall maximum amplitude;

3. there are short vertical wavelengths of circa 35 km in winter and longer values (>100 km) or evanescence in summer above ∼80 km, with modestly shorter wavelengths (60–100 km) in the fall above ∼80 km. However, below ∼80 km during the equinoxes and summer, the tidal wind wavelengths are smaller (circa 35 km).

These results are of course consistent with earlier CUJO papers (Manson et al., 2003, 2004a) where the data are presented in alternate complementary fashion. It is worthy of note, as remarked by one of the reviewers (a tidal specialist) of this Comment paper, that the direct phase-parameter measured is the vertical phase-gradient (degrees per km), and that conversion of this number into a vertical wavelength can be problematic when the height interval used is smaller than the calculated wavelength. While use of the latter is common in published tidal papers, we generally begin our papers with comments on the magnitude of the phase gradients, and note the equivalence to a wavelength (often giving the km-value in brackets); PETAL09 generally also follows this convention. While the community is generally aware that local gradients/inverse-wavelengths may be due to Hough mode superpositions, or even non-migrating tides (NMT), it is important to repeat this warning. The heights over which phase gradients are calculated for the MFR usefully range from 21–33 km (Manson et al., 2006). For numerical comparative simplicity, we will often use "vertical wavelengths" for the rest of this paper. Our general conclusion is that (i) at Yamagawa (31° N, 131° E) the DT-wind dominates; at Wakkanai, Platteville and London the SDT-wind and DT-wind intensities are quite comparable; while at Saskatoon the SDT-wind dominates; and (ii) at mid-latitudes and at heights near 85 km, for the SDT, the migrating tidal wind (s=2) is dominant, especially when the tide is large in the equinoxes and

winter. We note that the Platteville radar is ∼70 km away from Fort Collins, so that allowing for the field of view of the systems they are effectively coincident observing locations.

Remote sensing instruments on board satellites have made possible the delineation of nearly global distributions of tides. From HRDI-UARS wind observations, Manson et al. (2002c) obtained the global distributions of D and SD tides at ∼96 km for June–July (1993), December–January (1993/1994) and September–October (1994). The SDT-wind maximized near 40–55 degrees in winter and fall, and exhibited more modest longitudinal amplitude variations than the DT-wind. Using the same data archive, Manson et al. (2004b) discussed the zonal wave numbers for the 96 km tidal winds as functions of latitude. For the SDT-wind, the dominant migrating (s=2) tide, as well as nonmigrating tides with wave numbers s=−2, 0, 4, were demonstrated; the migrating tidal wind amplitude-maxima occur at latitudes poleward of 24°, and seasonal variations of hemispheric maxima plus symmetry or antisymmetry of EW/NS phases indicated the dominance of symmetric Hough modes, e.g. (2,4), (2,6) in the fall, plus (2,5) in the solstices.

Jacobi et al. (1999) examined the monthly variations of the SDT-wind at heights near 90 km, over the years (1985–1995), using 6 radars (3 were MWR) at 5 European and Russian locations between 52–56° N, and including Saskatoon (MFR) in Canada (52° N, 105° W). The variations of the SDT-phase and amplitudes, using monthly means at 92.5 km, were quite similar to those at 40° and 52° N in North America: winter and late summer-fall maxima of comparable amplitudes; and transitions of vertical phase-gradient between summer and autumn (equivalent to "vertical wavelengths…of… >100 km … ∼50 km" respectively). From Riggin et al. (2003), Poker Flat (65° N) and Andenes (69° N) observations from 1999–2001 showed that there is a clear repeatable enhancement in SDT-wind amplitudes around the autumn equinox for altitudes around 86 km and that during June–September the migrating SDT-wind is dominant at these latitudes. In the Southern Hemisphere (SH), the seasonal variations were more complex and the autumnal maximum less pronounced. They showed, using tidal theory that refraction of the tide in the hemispheric wind circulation could explain the NH late-summer/early autumn enhancements.

The conclusions from these earlier published radar data (40–55° N) from Europe, Russia and Canada is that the "vertical wavelengths" for the SDT tidal winds in summer months (June, July, August) above 80 km are long (∼100 km) or evanescent. This is in agreement with the thermal tides of YETAL08 at Fort Collins 41° N (who are referenced by PETAL09), but in disagreement with the SABER thermal migrating SDT vertical phase-gradients and thence "vertical wavelengths" (∼35 km) for 80–100 km, which are shown and discussed by PETAL09. We will next show new seasonal contour plots for the latitudes from 40 to 52° N.

3 Hemispheric ground-based observations of the late summer/early fall (LSEF: August–September) maxima for the SDT-wind amplitudes

There is evidently significant published evidence for the strong presence of LSEF maxima in the north-south (NS) and east-west (EW) wind components of the SDT. In preparation for this section we have reanalyzed much of the data used in the papers referenced above and also sought and analyzed additional data. The format used, and shown later for the Platteville and Saskatoon locations/MFR, involves thirty-day fits for the 12 and 24-h tidal wind oscillations and means at each radar location. The fits have the 15th day of the month at their mid-point, and contours on the time versus height plots result from a bilinear interpolation procedure (Manson et al., 2006). The zonal and meridional (tidal) amplitudes and phases were again assessed, with focus upon the LSEF feature as well as the relative winter maxima. Northward and eastward tidal winds are taken as positive, and the phases are the local solar times of maximum northward and westward winds (Fig. 1). We were the first users of MFR data to estimate and hence limit the height of presented winds/tides in published figures (Namboothiri et al., 1993), to locations *below* where radiowave group-retardation becomes large enough (greater than ∼3 km) to reduce the accuracy of assigned heights. Thus the tidal data at upper heights (>91 km) in summer are excluded in our figures. The effects of the increased ionization due to the "winter anomaly" (Manson, 1981; Garcia et al., 1986) were also generally considered in the production of contour-plots of amplitudes and phases of the semidiurnal tides as functions of height and time i.e. as in Manson et al. (2006) and earlier papers referenced there. In fact, the winter anomaly was found to have a positive influence on the MFR by enhancing the quantity of day-time data during winter in the lower D-region/upper mesosphere (Manson and Meek, 1987). Otherwise, no evidence for MFR radar group-retardation was found in the above papers for winter months e.g. variations in vertical phase-gradients of the SDT would be an indicator of this, and comparisons of phases between MFR and MWR winds are mentioned twice in discussions below.

The semi-diurnal tidal wind LSEF feature at NH latitudes is noted at latitudes as low as 31° N (Yamagawa; also see Igarashi et al., 2002). It begins there in August (as low as 85 km), maximizes in September (82–97 km) and only occurs above 90 km in October: the NS perturbations are larger than the EW. From 40–45° N the CUJO radars plus Urbana each show similar strong features and we show Platteville-contours for the years 2001–2007 in the bottom half of Fig. 1: heights as low as 73 km are available and the amplitudes of the LSEF feature begin near there. The maxima occur in August–September for the NS-wind and September for the EW; as noted before the phases are minimally changed in those months from the earlier summer-months. For Wakkanai (2000–2001) the LSEF maximizes in

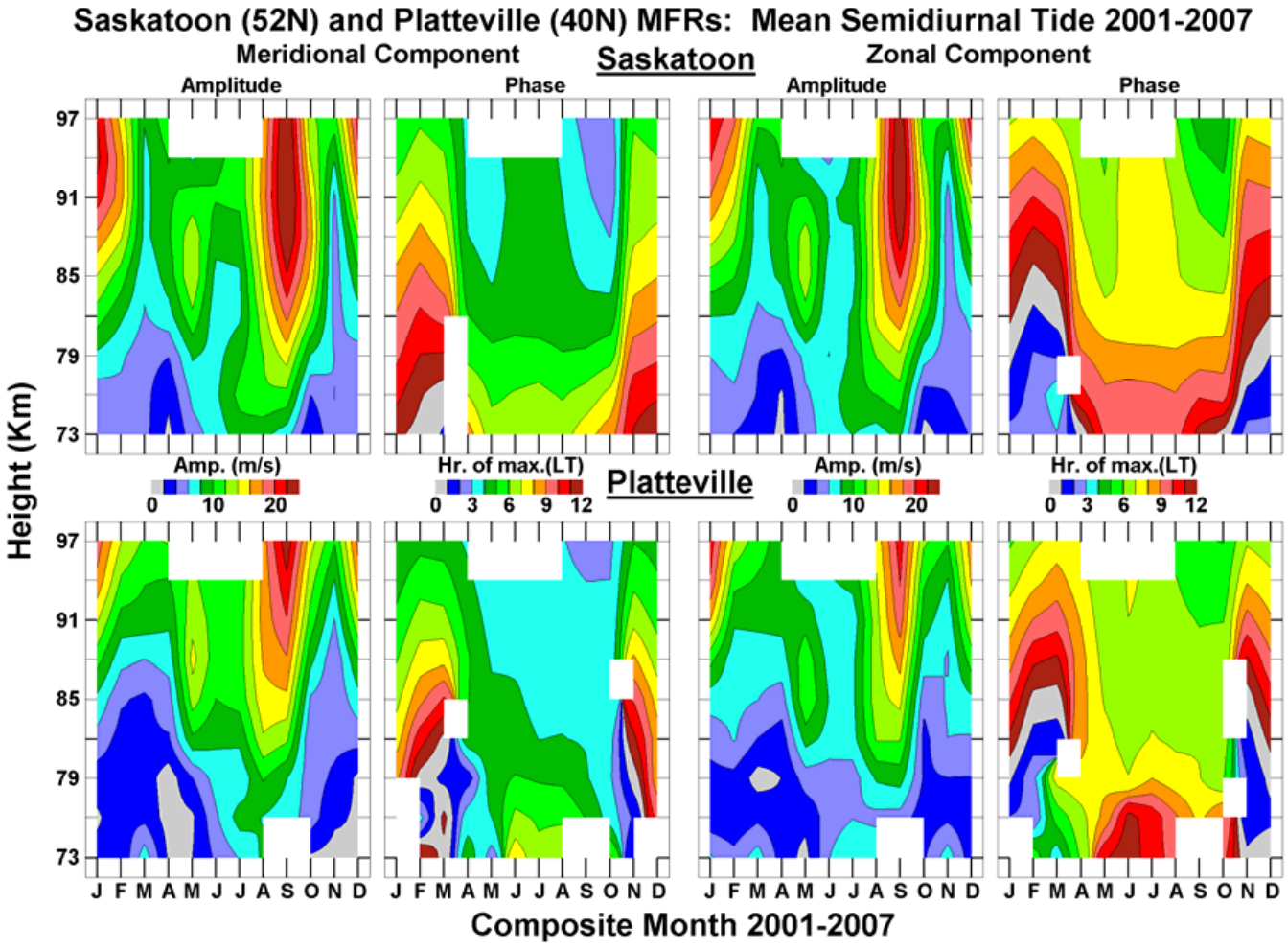

Fig. 1. Contour-plots of amplitudes and phases of the semidiurnal tide [meridional and zonal wind components] as functions of height and time: Data from Saskatoon and Platteville for the years 2001–2007 have been used.

September for EW and NS winds; and in August–September at Urbana (1991–2000) for both wind components. We acknowledge the role of Professor Steven Franke (University of Illinois at Urbana-Champaign) in his oversight/leadership of the MFR at Urbana, and the archiving of those 10 years of data.

A comment on the magnitude of the well known speed-bias for the MFR is appropriate, since this can affect the relative magnitudes of the SDT-winds within the mesopause-maxima of winter and the LSEF feature, as measured with MFR systems. This is also important when longitudinal variations of tides are assessed. Hall et al. (2005) compared the wind vectors from the collocated MFR and the MWR at Tromso (70° N), and their scatter plots provide the following numbers: the MFR speeds are smaller than the MWR by <10% below 88 km, 25% for 88–91 km, and 35% for 95 km (i.e. MWR/MFR=1.54). Phases/directions of the wind vectors were in very good agreement, as also noted in several references provided in their paper; this is consistent with an absence of group- retardation effects during winter in the MFR data. In an earlier such paper, Manson et al. (2004c) compared speeds from the Andenes/Tromso-MFRs and the Esrange-MWR, which is only 200 km south-east. Speed-ratios were tabulated for the first time by months as well as height: the MWR speeds were larger than the MFR by median-factors of 1.21 in summer, 1.31 in September and 1.75 in winter for the altitude range 94–97 km. Phases of the SDT winds, and their vertical gradients, were in very good agreement in each season; this is also consistent with an absence of group-retardation (winter anomaly) effects in the plotted MFR data. To conclude this discussion of possible radar biases, we note that a literature/office-search, conducted while in final review of this paper, revealed the recent and highly relevant paper by Jacobi et al. (2009). In this, they contemporaneously compare winds (2004–2005) from Juliusruh (MFR) and Collm ("Low Frequency" radiowave system), which featured in the Jacobi et al. (1999) paper, with data from the new Collm-MWR. The proximity of the three systems, and their antenna beam-widths, justifies such comparisons. They show that the MWR-winds are "generally

stronger than" MFR-winds, that the differences are "small near 80 km but increase with height", and that those differences are "larger during winter than during summer". Their MWR/MFR ratios (factors) for winter months at 94 km are larger, at typically 2.0–2.5. They suggested that the larger gravity wave fluxes during winter months could affect the MFR data. Their overall conclusions are entirely consistent with the material and discussion above, from Manson et al. (2004c).

Returning to Fig. 1, the figure also includes the SDT-wind contour-plots for Saskatoon, one of the radars within 50–56° N used by Jacobi et al. (1999). For Saskatoon the maximum of the LSEF feature is centred on September, and the vertical phase-gradients are modestly larger, especially above 85 km, than those at 40° N. Notice also that the tidal-wind phases at both locations are consistent with short vertical SDT-wind "vertical wavelengths" (circa 35 km) in winter-centered months, November to March; with large values (>100 km)/evanescence above 80 km in the late spring and early autumn months; and evanescence above ∼80 km in the summer (June, July, August). Below 80 km in the equinox and summer months the "vertical wavelengths" are smaller (circa 35 km), an observation that is unique to the MFR radars, due to their high sensitivity and hence data-yield at low altitudes. Finally, there is a matching but much smaller feature in late spring/early summer that is evident at 40° N and 52° N, and in both wind components; the tidal wind phases also respond to this. Simply applying the speed-biases from Manson et al. (2004c) in the previous paragraph, as corrections, the actual LSEF feature of the SDT for Saskatoon is likely to reach ∼31 m/s (∼96 km) rather than the 24 m/s shown in Fig. 1, which further emphasizes the significance of the SDT feature; while the winter maximum in January, which reaches slightly lower MFR-speeds, is likely to be closer to 38 m/s. These values are based upon the use of the MWR as a wind-speed standard, and apply for the interval 2001–2007 near 105° W. However, the LSEF feature there reaches higher speeds than in winter at altitudes below 90 km.

One further comment is appropriate to the SDT wind radar data from Urbana (40° N), and its relationship to the tidal *wind* lidar data from Fort Collins. YETAL08 show in their Fig. 4 a comparison: the tidal phases at 90 and 96 km agree extremely well, despite the sites' difference in longitude and the years involved in the plots; the amplitudes from the two instruments also both show an August–September maximum, and there is the expected bias (smaller) for the MFR radar at 96 km. This plot emphasizes the predictability of the LSEF feature and, along with the CUJO papers, the occurrence of the feature from eastern United States to Japan (150 degrees of longitude). As an aside, since this becomes important for later discussion, the LSEF feature of amplitude enhancement is seen in both the thermal and wind SD tide at Fort Collins 40° N.

To complete this section, we comment upon the radars in the 50–60 degree north sector (Jacobi et al., 1999) and then the range of longitudes from which SDT data are available from ground based systems. The radars observing the strong LSEF feature stretched from Saskatoon (107° W), through Collm (51° E) to Kazan (49° E). Thus the LSEF feature is regularly observed by radars in the 40–56° N latitude-sector westward from Japan to West-Central Russia: the longitudes missing are over Eastern Russia, Mongolia and Northern China (circa 90 degrees). However, the paper by Zhao et al. (2005), that uses observed winds from an MWR at Wuhan, China (31° N, 114° E), show the presence of SDT amplitude-maxima in August–September (as at Yamagawa). The feature is at its weakest near 30° N (Sect. 2), so its presence there indicates the likely global presence of this significant and interesting SDT feature. We have recently used data from the MWR and MFR at Collm (51° N, 13° E) and Saskatoon, respectively, for correlation-studies between the tides, migrating and non-migrating (MT, NMT), and stationary planetary waves SPW (Xu et al., 2009). There, we show that the MT dominates the NMT during the month of September 2006 when the LSEF feature occurs. Also, the vertical wavelengths of the SDT winds during summer months at Collm are also long or evanescent above 80 km. Finally, in the process of preparing this latter paper, and also another on high latitude tides (Manson et al., 2009), it became clear that the winter SDT tides above 85 km from the Collm-MWR are generally larger than those from the Saskatoon-MFR, even when the statistical speed-bias correction factor of 1.75 had been applied. The factor is closer to 2.0–2.5 above 90 km. Processes involved in such winter-months' longitudinal asymmetry are being sought; thermal and dynamic processes leading to the presence of NMT, as well as the causes of speed-biases, are possible candidates. Note that although at Collm the winter SDT (88–94 km) is also larger than the LSEF feature (as at Saskatoon when the correction factor is applied), the LSEF feature is strong (comparable with that at Saskatoon) and spatially/temporally distinct.

This section has shown that the late summer/early-fall (LSEF) SDT-wind amplitude maximum is a dominant annual feature in the mesosphere from 75–95 km km, and is larger than the winter maximum (December–February) below 85 km e.g. Fig. 1, at least for latitudes from 40–56° N in the Canada-US longitude sector. Excellent comparisons between the radar winds at Urbana (40° N) and the lidar winds and temperatures from Fort Collins (41° N) confirm that these two instruments see the same amplitude-feature in the SDT (YETAL08). Hemispheric radar SDT observations agree that the "vertical wavelengths" (λ_z) calculated from observed phase gradients (over 21–33 km height intervals) of the SDT are relatively small (λ_z circa 35 km) in winter, and larger (λ_z circa 100 km) or evanescent in summer above ∼80 km, with only modestly shorter "wavelengths" (60–100 km) in the fall. However, below ∼80 km during

the equinoxes and summer, the SDT "vertical wavelengths" are smaller (circa 35 km). Finally, calculations based upon the observed semi-diurnal tides from the CUJO radar network in the Japan-Pacific-North America longitudes, from the Saskatoon-Collm radar pair covering Canada-Western Europe, as well as the HRDI global tidal winds (all discussed in Sect. 2), agree that the migrating SDT (MT) is dominant over the non-migrating tides (NMT) during the time interval (August-September). This paragraph confirms and elaborates upon the shorter statement made by PETAL09 regarding *"the September maximum detected at northern middle latitudes... (by) radars"*... the latter of course are tidal winds while the SABER tides are thermal. The remaining question regards the possible differences between characteristics of the SDT wind and temperature perturbations. Are there latitudinal and altitudinal differences, which could explain the SABER results shown by PETAL09? We use the paper by YETAL08 and data from CMAM operating with data assimilation (DAS) to assess this matter in the next section.

4 Modelling and analysis methods

The purpose of this concluding section is to consider very briefly the materials available on the latitudinal structure of the mesopause SDT field perturbations, and therefore the inherit assumption of PETAL09 that amplitude structures observed (at some latitude) in the SDT temperature field will also exist in the dynamical fields, in particular the horizontal winds (zonal, EW, meridional, NS).

Comparisons of height versus SDT amplitude/phase profiles for latitudes of 0, 18, 42 and 60 degrees, from a then sophisticated numerical tidal model, were shown in the seminal paper of Forbes (1982). This early model already demonstrated that for the mesopause region the largest temperature, T, perturbations occurred at lower latitudes than for the EW and NS winds. Also, Hough mode extensions (HME; e.g. Forbes et al., 1994) have been used to provide tidal perturbations for winds, temperatures and densities at other heights and latitudes when the amplitude and phase of the wind field for a given HME is known for one height and latitude. Forbes and Wu (2006) showed the convincing consistency of the global temperature-structure at 86 km for the diurnal tide's NMT (s=−3) as observed by MLS (Micro-wave Limb Scanner, UARS), and the temperatures derived from HME using the observed winds at 95 km from UARS (Upper Atmosphere Research Satellite), WINDII (Wind Imaging Interferometer) and HRDI (High Resolution Doppler Interferometer). Summarizing, this again emphasizes that, from observations of seasonally varying tidal temperature perturbations at a given latitude, one may not presume the existence of similar variations of tidal wind perturbations at that same location.

Most recently, the paper of YETAL08 is outstanding in many respects, and some of its contents have been discussed above with respect to the paper of PETAL09. In addition they used the HAMMONIA chemical-climate model for 0–250 km (Schmidt et al., 2006) for location-specific comparisons with the Fort Collins sodium-lidar temperatures. Twelve months of profiles (80–100 km) were in excellent agreement for the phases, and the amplitudes were generally good, although HAMMONIA underestimated the equinoctial values, including the late summer/early fall (LSEF) feature of particular interest in this Comment paper. They also used the HAMMONIA data along with the lidar winds and temperatures to calculate the vertical wavelengths of the SDT, as well as the relative importance of the major Hough modes of the migrating SDT: the tidal wavelengths were shown to be shorter, in the height range 80–100 km, during winter (dominance of mode 2, 4) than in summer (dominance of modes 2, 3; 2, 2). Also the SDT MT of the mesopause region at 41° N was shown to be dominant over the NMT, except during October. (These last two conclusions are consistent with the papers using radar data that were discussed in the Introduction and Sect. 2). Finally there seems to be no physical reason why the vertical wavelengths (and also estimates of the dominant SDT Hough modes) at 41° N, as obtained from the lidar measurements and HAMMONIA, would be sensitive to the (2, 2; 2, 3) Hough modes in summer (YETAL09), while the SABER system (hardware and software) would in some unexplained fashion detect only the (2, 4; 2, 5) in summer months (PETAL09). The related quotation from the latter paper was provided in the Introduction.

We move finally to new results from the Canadian Middle Atmosphere Model (CMAM, Manson et al., 2006). At this time the Data Assimilation System (DAS) has been developed as an option (Ren et al., 2008), and results for the year 2006 are being used here. Data from models with DAS are much preferred to models with only climatological tropospheres, as CMAM without DAS did not typically produce realistic or timely mid winter stratospheric warmings (Manson et al., 2006), or indeed the equatorial quasi-biennial oscillation. We have selected DAS analyses for the 12 months of 2006, with additional attention paid to September, since that is a focus of this Comment paper. As the reader will now perceive, the LSEF/"September" feature is a dominant amplitude feature of the SDT mesopause-wind field (modestly smaller or greater, depending upon height, to that of winter) as observed by radars (within 40–56° N, and a hemispheric range of longitudes) and lidar, and must also be seen as such from remote sensing by satellites. Also, as noted in the earlier sections the agreement between the CMAM tidal windfield without DAS and the radars at Saskatoon and Platteville was already very acceptable (Manson et al., 2006). CMAM-DAS provides even better agreement (below), and several years of such data will be discussed elsewhere in more detail.

Figure 2 provides the tidal meridional wind contour plots, time versus height, using the same plotting software as for Fig. 1. (The tidal wind contour plots for the zonal wind

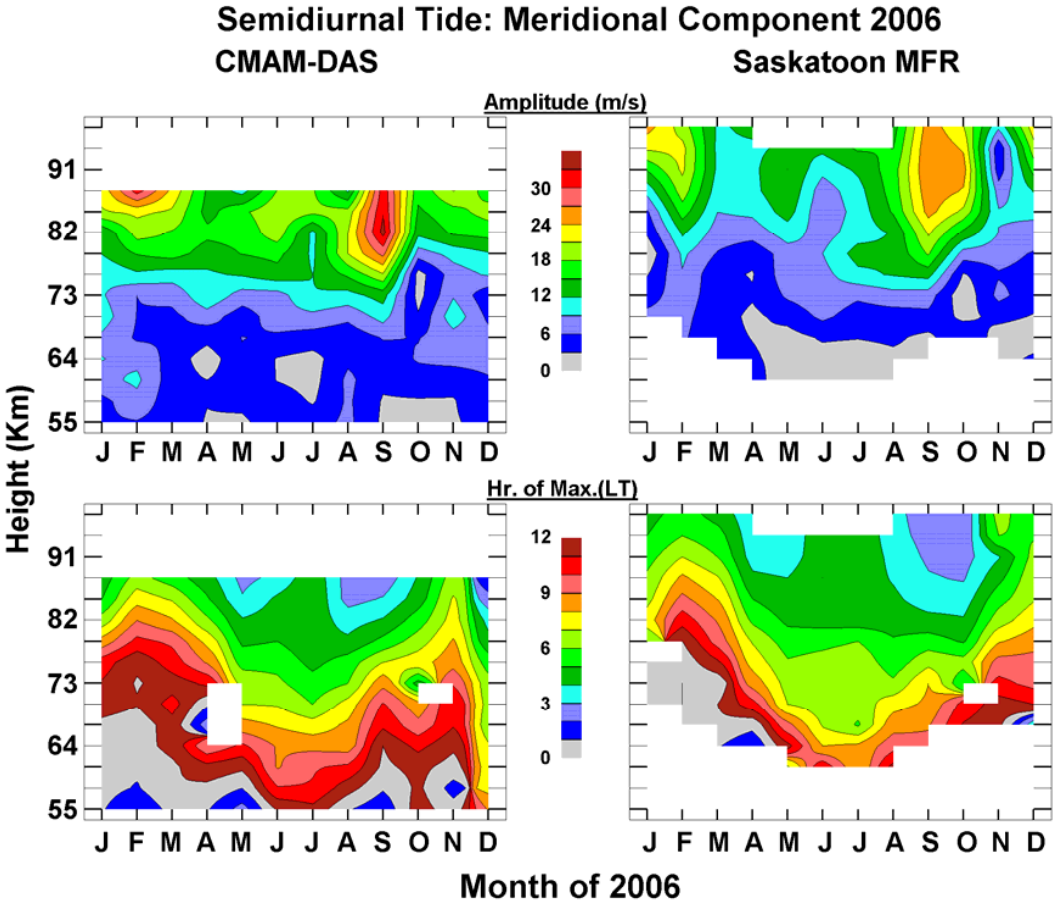

Fig. 2. Contour-plots of amplitudes and phases of the semidiurnal tide [meridional wind component] as functions of height and time: Data for 2006 from the Saskatoon MF radar and the model CMAM-DAS at this location (105 W, 52 N) have been used. Please see the text for any additional details.

component are not shown, but as expected from Fig. 1, the tidal characteristics are not component-specific.) Saskatoon radar data and CMAM-DAS data for the 2006 are used; since CMAM data for 96 longitudes and 48 latitudes are available, data were interpolated to Saskatoon (52° N, 107° W) and used to provide the location-specific model-data and hence tidal contours. Geopotential heights are used up to 88 km, which allows full global coverage for the tidal winds and wave-number spectra. The purpose of this figure is to illustrate the similarity between radar observations and the model at middle latitudes, evidencing enhanced agreements compared to earlier non-DAS results. This is so especially with the now larger modeled summer (June–August) vertical phase gradients, i.e. smaller "vertical wavelengths" of ∼35 km, below circa 73 km. Above there they are long or evanescent, as observed (Figs. 1 and 2). During the winter-centered months of Fig. 2 the wavelengths are modeled and observed (for 2006) to be 30–35 km. The plots from radar and model both show winter and September tidal wind amplitude-maxima, the later reaching to lower heights (∼75 km). The heights of the two maxima appear to be ∼3 km lower in the model, but that is likely due to color contour-changes associated with modestly smaller values for the radar (as calculated, without speed-bias correction), which is expected (Sect. 3). The phase values, with respect to both height and month, are remarkably similar for radar and CMAM, and we look forward to later detailed assessments of the tides (SDT and DT) and their forcings that are present in CMAM. Plots of contours from CMAM data for the migrating SDT (s=2) at 52° N (not shown) are very similar to the location-specific contours of Fig. 2, with the LSEF feature being dominant over the year, especially below 82 km. The plots for Platteville (radar and model) were very similar to Fig. 2, but we show the Saskatoon radar data as they are of better quality and quantity for this single year example. The observations, of the wind perturbations at least, based upon 7 years of data (Fig. 1), indicate clearly that the SDT observed amplitudes and phases are very similar at 52° N 107° W and 40° N 105° W. The observed (SABER) SDT migrating thermal tides (PETAL09) also show only modest changes between 40 and 50° N; but our next two figures are height versus latitude contour-plots (pole to pole), so any latitudinal

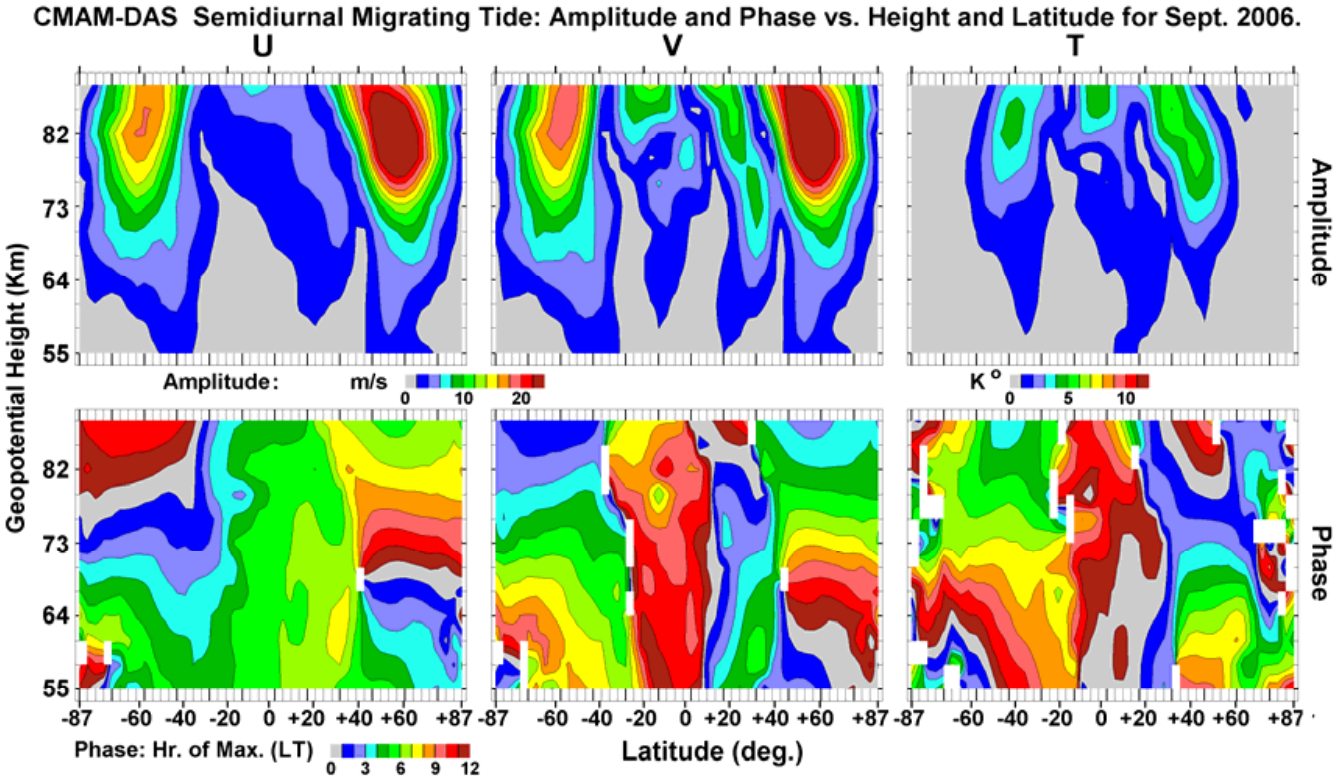

Fig. 3. Contour-plots of amplitudes and phases of the migrating (s=2) semidiurnal tide [meridional and zonal wind components, and temperature] as functions of height and latitude: data for September 2006 from the model CMAM-DAS have been used.

variations in the modeled tide (winds and temperatures) are also available.

Thus, Fig. 3 provides the global CMAM-DAS amplitudes and phases for the migrating SDT for the month of September 2006; the east-west (U) and north-south (V) winds are shown, but now also the thermal tides. From inspection of such height versus latitude plots for all months of 2006 (not shown), we confirm that for heights near 80 km the tidal winds (EW, NS) and temperature perturbations of the Northern Hemisphere (NH) both have maximum mid-latitude values for the year in September, especially below 85 km, given that the feature extends to lower heights than the winter maxima for both model and radar. From Fig. 3 the LSEF wind feature is dominant from 35–75° N, and above ∼73 km. Maximum amplitudes of ∼5 degrees are comparable to observations (YETAL08); and the color scale has been normalized to the maximum value for the year, which occurred near the equator (∼6° N, ∼10 Kelvin near 85 km). The corresponding vertical phase gradients are large from 64–88 km ("vertical wavelengths" are ∼30 km at low altitudes and increasing modestly with height), which are unlike those in summer (June–August, Fig. 2) when the phase gradients are smaller above ∼73 km ("vertical wavelengths") of ∼100 km or evanescent). Of great significance for this Comment, the thermal tides have maxima at 30° N and a lesser maximum at the equator, and would be visible, i.e. observable with any adequate system, from 20–50° N. The vertical wavelengths are also small there, at 30–35 km throughout the mesosphere.

Regarding the latitudinal structures, the global wind amplitudes and phases of Fig. 3 are consistent with the (2, 4) Hough mode (Forbes, 1982): the maxima are at middle latitudes (∼50 degrees); the EW winds are symmetrical in phase about the equator; and the NS winds are anti-symmetrical in phase about the equator and there are smaller amplitude peaks near 15 degrees. The lack of symmetry in amplitude and phase beyond 40° N/S could be due to the effects of both NMT and asymmetric Hough modes such as (2, 5); our recent Hough mode analysis of the year 2006 shows relatively large (2, 5) amplitudes compared with neighboring months. Consistent with this, and as discussed in an earlier paper (Chshyolkova et al., 2006), the fact that dynamically the winter seasons are longer (7 months) than summer will lead to such equinoctial hemispheric asymmetries. The latitudinal structures of the thermal tides are much more complex, and simple diagnosis is no longer possible here. These will be treated elsewhere in a more substantial paper; there is evidence for both symmetric and asymmetric modes and superposition of lower and higher order Hough modes. For our purpose here, it is enough to note that in a GCM of considerable sophistication and with DAS, the latitudinal thermal

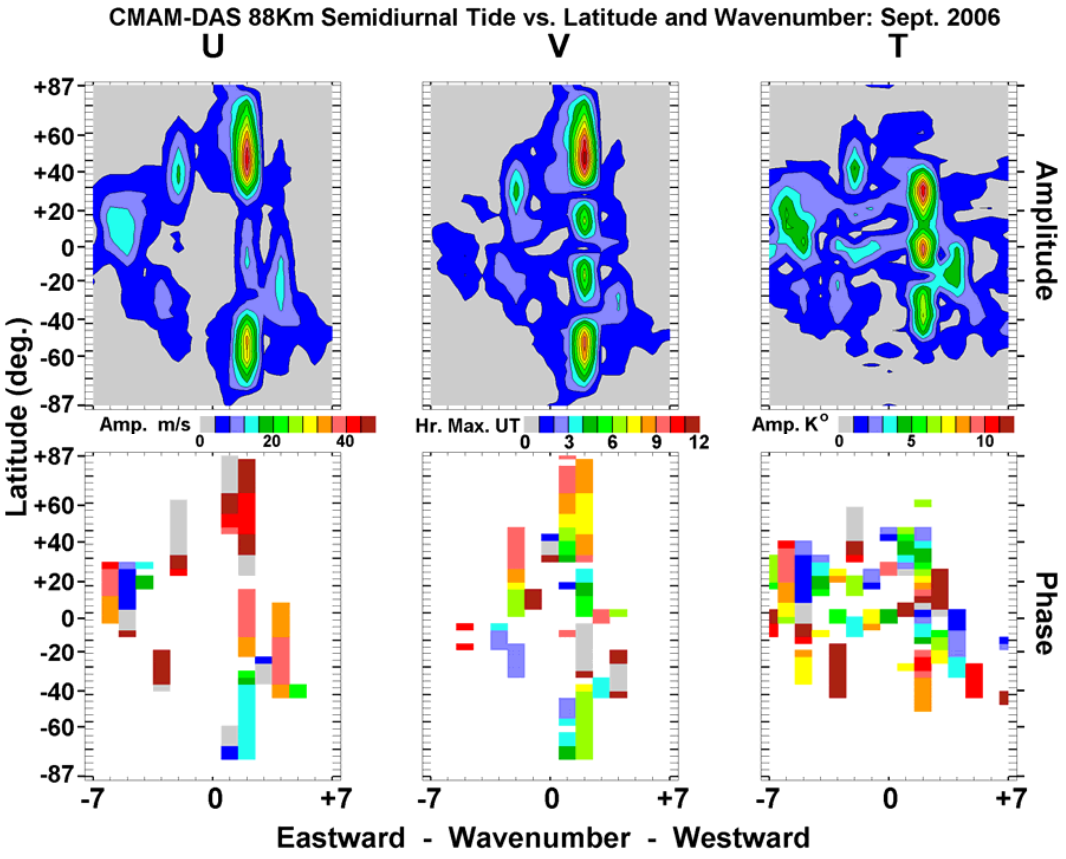

Fig. 4. Contour-plots of amplitudes and phases of the semidiurnal tide [meridional and zonal wind components, and temperature] as functions of wave-number and latitude: Data for September 2006 from the model CMAM-DAS have been used, and the results for 88 km are shown.

tidal structure is significantly different from that of the wind field. The absence of recognition of this in PETAL09 is of concern; and their claims of similarity between thermal and wind SDT features in their "Discussion and Summary" were instead used to bolster the validity of the SABER tides in general.

Finally we show in Fig. 4 the wave-number spectra for the SDT within CMAM-DAS at 88 km and for September 2006. In the Northern Hemisphere the MT is clearly dominant (m=+2, westward), and the largest NMT is m=−2, consistent with forcing by a stationary planetary wave, or latent heat released in the troposphere (Hagan and Forbes, 2003; Manson et al., 2004b). The wave-number of this forcing is therefore S=4 and is likely due to the latent heat process (Manson et al., 2009); its presence is verified in CMAM by the existence of NMT m=−3 for the diurnal tide (not shown). The SDT is well behaved globally, as the meridional (northward) leads the zonal (eastward) in the NH, and the reverse in the SH. The thermal tide's latitudinal preference for maxima is again underscored, so that it is merely fortuitous that at ∼40° N both the wind and thermal tides can both be recognized or observed within the spectral window (temporal, spatial) of an experimental system.

5 Conclusions

These will be relatively short, as the reader will have followed the development of this Comment and recognized that the authors' initial concerns regarding the differences between thermal and wind perturbations associated with the semidiurnal tide (SDT), and between analytical tidal results from ground based (radar, lidar) and space based (SABER) systems, were justified.

It has been confirmed, using radar and model data from well distributed longitudes, that the September SDT wind feature (here abbreviated as the LSEF) is one of the two dominant annual features (the other being winter's lower thermospheric SDT) at middle latitudes 40–60° N and at heights of 75–90 km. Spatial spectral analysis applied to radar data in Pacific-North America and Europe-Russia sectors, and also to hemispheric data from the sophisticated GCM (CMAM-DAS; Data Assimilation System), has indicated that the migrating tide (MT) is dominant. Thus, comparisons of the MT for the semi-diurnal oscillation of a particular atmospheric variable (e.g. coming from satellite data) with locally observed tides are justified, and indeed close similarities are expected in this case. This statement would have to be for

the thermal tide on the one hand, and the wind-tide on the other.

However, we have shown by using CMAM-DAS, which provides very good agreement with the observed semi-diurnal wind-tide at 40° N and 52° N (Platteville-USA and Saskatoon-Canada), that the thermal tide has significantly different latitudinal variations throughout the mesosphere than does the wind-tide. For example the migrating thermal tide peaks at 30° N, while the migrating wind-tide peaks at 50° N, at heights above 70 km. Also, spectra for each month of the year indicated that the thermal and wind-tides provide the largest dominant annual values below 88 km in September. A significant quantity of high quality ground-based observations at Colorado-USA (40/41° N, Platteville and Fort Collins) have facilitated this present study (e.g. Yuan et al., 2008) and this Comment, as both temperature and wind-tides have been successfully observed there with good instruments. The tidal peaks are sufficiently broad in latitude to enable this. It is therefore very important that tidal papers clearly and frequently (text, figure captions) remind the reader that statements are being made with regard to a thermal or wind-tide. For example, observations may be made at latitudes where the wind or temperature perturbations are negligible, and their absence in one field may simply be because one is at a node for the appropriately dominant Hough mode. Our concern on this matter was aroused with the recent paper by Pancheva et al. (2009) (PETAL09), where references to radar, lidar and SABER data were made.

Specifically, the claim is made in the "Discussion and Summary" of PETAL09 that "*between 70 and 90 km... an autumn (September in the NH...) tidal amplification is evident as well. The September maximum... well documented by radar studies....*" This feature is not evident in the monthly height contours of thermal tides for 40° N in their Fig. 2 (there is instead a uniform light grey (2–4 degrees) from August to November–December), or in the 90 km monthly time sequence of amplitudes over six years in their Fig. 3. The average (2002–2007) monthly time sequence at 90 km, and for 40° N, show only a minimal upward departure from a straight line joining the August and October values in Fig. 4. Indeed, as noted in the Introduction, the 41° N lidar observations of the thermal tide by Yuan et al. (2008) (YETAL08) demonstrate a semi-annual feature, which involves amplitude maxima in the LSEF and spring time intervals... the smaller spring enhancements and phase changes are evident in our Figs. 1 and 2. Neither the tidal analysis of SABER data, nor the text of PETAL09, provides indications of this observed semi-annual variability.

The 60 day data-window that is slid by one day (PETAL09) will broaden an amplitude feature having duration of approximately one month (Figs. 1, 2) by a factor of approximately two, depending upon the definition of a maximum. For example we recalculated the twelve month SD tidal-wind contour plots using a 60 day window, and the strong maxima/minima of September/November were only very modestly changed; with the color format of Fig. 1 the change was difficult to discern. Hence, the October–November minimum is still expected to exist in contours of the thermal tidal field, or at the very least the smoothing could move the peak of winter (December–January) backwards in time toward the autumn. The effect will of course depend upon the relative magnitudes of the September and winter maxima as functions of height. We have also run the spectral program used for Fig. 3 with a 60 day window instead of 30 days, for each interval centered on the middle of each calendar month. The result was as expected: the September SD thermal maximum of the NH decreased modestly (the 5–6 Kelvin contour of yellowish green in Fig. 3 was removed) but no change occurred in the contours of lower temperatures (∼3 Kelvin) distinguishing October–November, so the temporal and spatial maximum of the LSEF/September was retained. The vexing question therefore remains for the NH semidiurnal tides discussed in this Comment: why is the "September" thermal and wind tides' amplitude feature, which exists dominantly in the middle latitude mesosphere-lower thermosphere (∼75 to over 90 km) as indicated by data from longitudinally well spaced radars of several types, a lidar, and the sophisticated General Circulation Model CMAM with data assimilation, not evident in the thermal SD tides derived from SABER data?

Further, the radar (meteor and medium frequency) and lidar observations from earlier publications, new presentations provided in this Comment, and the CMAM-DAS for 2006, show unambiguously that the "vertical wavelengths" (derived from vertical phase-gradients) of the SDT (either the migrating or locally observed tide, thermal or wind-tide) are relatively long (circa 100 km) or evanescent during the summer months from 80–100 km. This is in strong contrast to the wavelengths (∼35 km) provided in PETAL09 for the migrating thermal tide at latitudes of 40–50° N. Also, as noted in the Introduction, they state the following in their "Discussion and Summary": ..."*while for the lidar semidiurnal tide the Hough modes with very long vertical wavelengths (2, 2) and (2, 3) are dominant in summer the SABER tide is composed by modes with significantly shorter wavelength as (2, 4) and (2, 5) modes.*" Hough modes are a mathematical construct used to explain or organize the latitudinal and altitudinal structures of the observed tidal fields. With adequate vertical resolution (and the radars, lidar and SABER can and do each resolve 30 km structures with ease) and enough horizontal resolution to resolve the larger scales (greater than 2000 km) of latitudinal Hough mode structures (radars and lidars provide circa 300 km spatial averages and SABER circa 500 km) each system will provide information on the actual and existing tidal structures... and hence inherent Hough modes. These actual semi-diurnal (SD) tidal structures, which may be described by combinations/superpositions of the complex Hough modes, may be dominated by a particular Hough mode for a given month and height, or maybe a combination of modes. Given the spatial resolutions of the systems

under discussion, there is no conceivable way in which the "SABER tide", which is obtained by atmospheric sampling from SABER, can be different from the "lidar (and radar) tide", which is obtained by sampling with the radars, lidar and model. . . unless either the satellite's temporal and spatial sampling, inversion processes or the subsequent analyses are problematic in some unexpected fashion.

In this regard, we have "flown" through the CMAM-DAS 2006 atmosphere, sampling as SABER did in that year. Comparisons of tidal spectral signatures (such as shown in the figures of this paper) using such sampling, with those obtained using the full model atmosphere, revealed a high tidal sensitivity to the low frequencies. Meek and Manson (2009) have explored the related complex issues of aliasing. Removal of the simple linear trend from such SABER-sampled data may not be sufficient to provide an unbiased/non-aliased product.

Acknowledgements. Funding for this work was from CANDAC-PEARL, in part from its IPY funding; the Canadian Natural Sciences and Engineering Research Council (NSERC); and the University of Saskatchewan through support to ISAS. We acknowledge with pleasure the CMAM-DAS team (University of Toronto and Environment Canada) for providing the model-data; they in turn acknowledge funding sources of CFCAS (Canadian Foundation for Climate and Atmospheric Sciences) and the CSA (Canadian Space Agency). We acknowledge with thanks the high quality reports provided by the two referees provided by the Topical Editor.

Topical Editor C. Jacobi thanks two anonymous referees for their help in evaluating this paper.

References

Chshyolkova, T., Manson, A. H., Meek, C. E., Avery, S. K., Thorsen, D., MacDougall, J. W., Hocking, W., Murayama, Y., and Igarashi, K.: Planetary wave coupling processes in the middle atmosphere (30–90 km): a study involving MetO and MF radar data, J. Atmos. Solar-Terr. Phys., 68, 353–368, 2006.

Forbes, J. M.: Atmospheric Tides 2. The Solar and Lunar Semidiurnal Components, J. Geophys. Res.-Space Phys., 87, 5241–5252, 1982.

Forbes, J. M., Manson, A. H., Vincent, R. A., Fraser, G. J., Vial, F., Wand, R., Avery, S. K., Clark, R. R., Johnson, R., Roper, R., Schminder, R., Tsuda, T., and Kazimirovsky, E. S.: Semidiurnal Tide in the 80-150 km Region: and Assimilative Data Analysis., J. Atmos. Solar-Terr. Phys., 56, 1237–1249, 1994.

Forbes, J. M. and Wu, D.: Solar tides as revealed by measurements of mesosphere temperature by the MLS experiment on UARS, J. Atmos. Sci., 63, 1776–1797, 2006.

Garcia, R. R., Solomon, S., Avery, S. K., et al.: Transport of Notric–Oxide and the D-region Winter Anomaly, J. Geophys. Res., 92(D1), 977–994, 1987.

Hagan, M. E. and Forbes, J. M.: Migrating and nonmigrating semidiurnal tides in the upper atmosphere excited by tropospheric heat release, J. Geophys. Res., 108(A2), SIA6, 1062, doi:10.1029/2002JA009466, 2003.

Hall, C. M., Aso, T., Tsutsumi, M., Nozawa, S., Manson, A. H., and Meek, C. E.: A comparison of mesosphere and lower thermosphere neutral winds as determined by meteor and medium-frequency radar at 70° N, Radio Sci., 40, RS4001, doi:10.1029/2004RS003102, 2005.

Igarashi, K., Namboothiri, S. P., and Kishore, P.: Tidal structure and variability in the mesosphere and lower thermosphere over Yamagawa and Wakkanai, J. Atmos. Solar-Terr. Phys., 64, 1037–1053, 2002.

Jacobi, C., Portnyagin, Y. I., Solovjova, T. V., et al.: Climatology of the semidiurnal tide at 52–56 degrees N from ground-based radar wind measurements 1985–1995, J. Atmos. Solar-Terr. Phys., 61, 975–991, 1999.

Jacobi, Ch., Arras, C., Kurschner, D., Singer, W., and Hoffmann, P: Comparison of mesopause region meteor radar winds, medium frequency radar winds and low frequency drifts over Germany, Adv. Space Res., 43, 247–252, 2009.

Manson, A. H.: Comments on "Morphological Features of the Winter Anomaly in Ionospheric Absorption of Radiowaves at Mid-Latitudes" by Teruo Sato, J. Geophys. Res., 86, 1633–1635, 1981.

Manson, A. H. and Meek, C. E.: Small Scale Features in the Middle Atmosphere Wind Field at Saskatoon, Canada (52° N, 107° W): an Analysis of MF. Radar Data with Rocket Comparisons, J. Atmos. Sci., 44, 3662–3672, 1987.

Manson, A. H., Meek, C. E., Hagan, M., Hall, C., Hocking, W., MacDougall, J., Franke, S., Riggin, D., Fritts, D., Vincent, R., and Burrage, M.: Seasonal variations of the semi-diurnal and diurnal tides in the MLT: multi-year MF radar observations from 2 to 70° N, and the GSWM tidal model, J. Atmos. Solar-Terr. Phys., 61, 809–828, 1999.

Manson, A. H., Meek, C., Hagan, M., Koshyk, J., Franke, S., Fritts, D., Hall, C., Hocking, W., Igarashi, K., MacDougall, J., Riggin, D., and Vincent, R.: Seasonal variations of the semi-diurnal and diurnal tides in the MLT: multi-year MF radar observations from 2–70° N, modelled tides (GSWM, CMAM), Ann. Geophys., 20, 661–677, 2002a, http://www.ann-geophys.net/20/661/2002/.

Manson, A. H., Meek, C. E., Koshyk, J., Franke, S., Fritts, D. C., Riggin, D., Hall, C. M., Hocking, W. K., MacDougall, J., Igarashi, K., and Vincent, R. A.: Gravity wave activity and dynamical effects in the middle atmosphere (60–90 km): observations from an MF/MLT Radar Network, and results from the Canadian Middle Atmosphere Model (CMAM), J. Atmos. Solar-Terr. Phys., 64, 65–90, 2002b.

Manson, A. H., Luo, Y., and Meek, C.: Global distributions of diurnal and semi-diurnal tides: observations from HRDI-UARS of the MLT region, Ann. Geophys., 20, 1877–1890, 2002c, http://www.ann-geophys.net/20/1877/2002/.

Manson, A. H., Meek, C. E., Avery, S. D., and Thorsen, D.: Ionospheric and dynamical characteristics of the MLT region over Platteville (40° N, 105° W) and comparisons with the region over Saskatoon (52° N, 107° W), J. Geophys. Res., 108(D13), 4398, doi:10.1029/2002JD002835, 2003.

Manson, A. H., Meek, C. E., Chshyolkova, T., Avery, S. K., Thorsen, D., MacDougall, J. W., Hocking, W., Murayama, Y., Igarashi, K., Namboothiri, S. P., and Kishore, P.: Longitudinal and latitudinal variations in dynamic characteristics of the MLT (70–95 km): a study involving the CUJO network, Ann. Geophys., 22, 347–365, 2004a, http://www.ann-geophys.net/22/347/2004/.

Manson, A. H., Meek, C., Hagan, M., Zhang, X., and Luo, Y.:

Global distributions of diurnal and semidiurnal tides: observations from HRDI-UARS of the MLT region and comparisons with GSWM-02 (migrating, nonmigrating components), Ann. Geophys., 22, 1529–1548, 2004b, http://www.ann-geophys.net/22/1529/2004/.

Manson, A. H., Meek, C. E., Hall, C.M., Nozawa, S., Mitchell, N.J., Pancheva, D., Singer, W., and Hoffmann, P.: Mesopause dynamics from the scandinavian triangle of radars within the PSMOS-DATAR Project, Ann. Geophys., 22, 367–386, 2004c, http://www.ann-geophys.net/22/367/2004/.

Manson, A. H., Meek, C. E., Chshyolkova, T., McLandress, C., Avery, S. K., Fritts, D. C., Hall, C. M., Hocking, W. K., Igarashi, K., MacDougall, J. W., Murayama, Y., Riggin, D. C., Thorsen, D., and Vincent, R. A.: Winter warmings, tides and planetary waves: comparisons between CMAM (with interactive chemistry) and MFR-MetO observations and data, Ann. Geophys., 24, 2493–2518, 2006, http://www.ann-geophys.net/24/2493/2006/.

Manson, A. H., Meek, C. E., Chshyolkova, T., Xu, X., Aso, T., Drummond, J. R., Hall, C. M., Hocking, W. K., Jacobi, Ch., Tsutsumi, M., and Ward, W. E.: Arctic tidal characteristics at Eureka (80° N, 86° W) and Svalbard (78° N, 16° E) for 2006/07: seasonal and longitudinal variations, migrating and non-migrating tides, Ann. Geophys., 27, 1153–1173, 2009, http://www.ann-geophys.net/27/1153/2009/.

Meek, C. E. and Manson, A. H.: Summer planetary-scale oscillations: aura MLS temperature compared with ground-based radar wind, Ann. Geophys., 27, 1763–1774, 2009, http://www.ann-geophys.net/27/1763/2009/.

Namboothiri, S. P., Manson, A. H., and Meek, C. E.: E Region Real Heights and their Implications for MF Radar-derived Wind and Tidal Climatologies, Radio Sci., 28(2), 187–202, 1993.

Pancheva, D., Mukhtarov, P., and Andonov, B.: Global structure, seasonal and interannual variability of the migrating semidiurnal tide seen in the SABER/TIMED temperatures (2002–2007), Ann. Geophys., 27, 687–703, 2009, http://www.ann-geophys.net/27/687/2009/.

Ren, S., Polavarapu, S. M., and Shepherd, T. G.: Vertical propagation of information in a middle atmosphere data assimilation system by gravity-wave drag feedbacks, Geophys. Res. Lett., 35, L06804, doi:10.1029/2007GL032699, 2008.

Riggin, D. M., Meyer, C. K., Fritts, D. C., et al.: MF radar observations of seasonal variability of semidiurnal motions in the mesosphere at high northern and southern latitudes, J. Atmos. Solar-Terr. Phys., 65, 483–493, 2003.

Schmidt, H., Brasseur, G. P., Charron, M., et al.: The HAMMONIA chemistry climate model: Sensitivity of the mesopause region to the 11-year solar cycle and CO2 doubling, J. Climate, 19, 3903–3031, 2006.

Yuan, T., Schmidt, H., She, C. Y., Krueger, D. A., and Reising, S.: Seasonal variations of semidiurnal tidal perturbations in mesopause region temperature and zonal and meridional winds above Fort Collins, Colorado (40.6° N, 105.1° W), J. Geophys. Res., 113, D20103, doi:10.1029/2007JD009687, 2008.

Xu, X., Manson, A. H., Meek, C. E., Chshyolkova, T., Drummond, J. R., Hall, C. M., Jacobi, Ch., Riggin, D., Hibbins, R. E., Tsutsumi, M., Hocking, W. K., and Ward, W. E.: Relationship between variability of the semidiurnal tide in the Northern Hemisphere mesosphere and quasi-stationary planetary waves throughout the global middle atmosphere, Ann. Geophys., 27, 4239–4256, 2009, http://www.ann-geophys.net/27/4239/2009/.

Zhao, G., Liu, L., Wan, W., Ning, B., and Xiong, J.: Seasonal behavior of meteor radar winds over Wuhan, Earth Planets Space, 57, 61–70, 2005.